analytical chemistry

pubs.acs.org/ac
Article

Liquid Chromatography Methods for Analysis of mRNA Poly(A) Tail Length and Heterogeneity

Martin Gilar,* Catalin Doneanu, and Maissa M. Gaye

Cite This: *Anal. Chem.* 2023, 95, 14308−14316
Read Online

ABSTRACT: Messenger RNA (mRNA) is a new class of therapeutic compounds. The current advances in mRNA technology require the development of efficient analytical methods. In this work, we describe the development of several methods for measurement of mRNA poly(A) tail length and heterogeneity. Poly(A) tail was first cleaved from mRNA with the RNase T1 enzyme. The average length of a liberated poly(A) tail was analyzed with the size exclusion chromatography method. Size heterogeneity of the poly(A) tail was estimated with high-resolution ion-pair reversed phase liquid chromatography (IP RP LC). The IP RP LC method provides resolution of poly(A) tail oligonucleotide variants up to 150 nucleotide long. Both methods use a robust ultraviolet detection suitable for mRNA analysis in quality control laboratories. The results were confirmed by the LC-mass spectrometry (LC MS) analysis of the same mRNA sample. The poly(A) tail length and heterogeneity results were in good agreement.

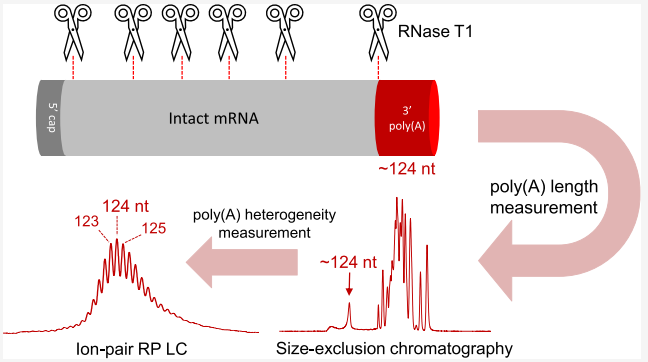

The first approved mRNA vaccines were deployed against SARS-CoV-2 virus.[1−3] Other therapeutic mRNA candidates are under clinical trials as vaccines, prophylactic cancer treatment, or protein replacement therapies.[4−6] The high level of interest in mRNA therapy research is motivated by mRNA technology's promising features, such as low toxicity, delivery via noninfectious agents, sequence-programmable in vivo target protein production, and inexpensive cell-free mRNA manufacturing.[7]

The first results of antitumor mRNA clinical trial were reported in 2008.[8] Since the emergency use authorization of COVID-19 mRNA vaccines on December 11, 2020, the number of mRNA clinical trials has increased significantly. Curreri and colleagues estimated that in 2021, about 222 trials employed RNA therapy; 53% were mRNA molecules.[9] Most mRNA clinical trials are in cancer treatment followed by infectious and genetic diseases. mRNA vaccines in development against infectious diseases are targeting Zika virus, rabies, respiratory syncytial virus (RSV), cytomegalovirus (CMV), and seasonal influenza.[7,9]

Rapid advances in mRNA technology require the development of novel analytical methods. USP draft guidelines[10] outline the attributes of therapeutic mRNA molecules that should be monitored. However, the application of existing separation methods is difficult due to the large size of the mRNA molecules. The length of therapeutic mRNA vaccines depends primarily on the size of the translated region encoding for the gene(s) of interest (GOI). COVID-19 mRNA vaccines coding for the SARS-CoV-2 spike protein are approximately 4400 nucleotides (nt) in length, while the vaccines encoding for two or more viral antigens or self-amplifying mRNA (saRNA) containing replicase genes[11] could be up to 12,000 nt long. This size of RNA is difficult to analyze by liquid chromatography (LC), gel electrophoresis (GE), or mass spectrometry (MS) methods.[12−14] Therefore, the analytical methods often utilize specific RNA nucleases to cut the mRNA molecules into more manageable oligonucleotides.[15−18]

The important features of therapeutic mRNA are the 5′-end-cap and 3′-end poly(A) tail.[19] The 5′-capping structure contains an N7-methylated guanosine linked to the first mRNA nucleotide via a reverse 5′ to 5′ triphosphate linkage.[20] Capping also includes 2′ O-methylation of the first mRNA nucleotide. This so-called Cap-1 structure facilitates the mRNA translation process by latching onto ribosomes in the cell.[20] 5′-capping is either performed cotranscriptionally via enzymes added to the reaction[4,20] or by incorporating the chemically synthesized Cap-1 structure post-transcriptionally.[21] The completeness of capping reaction can be measured by LC-MS of the 5′-end oligonucleotide cleaved from mRNA with RNase H or by other methods.[18,22,23]

Received: June 12, 2023
Accepted: August 28, 2023
Published: September 11, 2023

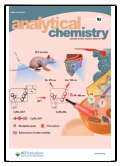

https://doi.org/10.1021/acs.analchem.3c02552
Anal. Chem. 2023, 95, 14308−14316

Next-generation sequencing (NGS) techniques are applicable to the analysis of the mRNA primary vaccine sequence.[24] Alternatively, LC-MS methods were proposed for mRNA oligo mapping and confirmatory sequencing.[15−17] Messenger RNA oligo mapping utilizes specific ribonucleases that cleave mRNA into shorter oligonucleotides. The RNA sequence coverage obtained from the unique mass of oligonucleotides is relatively low (30−81%) since many noninformative (short or isobaric) oligonucleotides are produced by the digest.[15,16] More complete sequence coverage can be obtained by performing several mRNA digests with different selectivity enzymes or by combining the mRNA mapping with MS/MS oligonucleotide sequencing. Both approaches require powerful data analysis software to make this a viable technique for the routine analytical laboratories.[15,25]

The 3′-end plays a critical role in maintaining mRNA in vivo stability. mRNA vaccines are cotranscriptionally or post-transcriptionally modified with a 100−150 nt poly(A) tail to enhance their half-life in vivo.[19,21] The length and heterogeneity of the poly(A) tail analysis are one of the quality control tasks proposed for inclusion in the USP guidelines. Even when the poly(A) tail is cleaved from the mRNA molecule, the length of the target oligonucleotides presents a challenge for the state-of-the-art separation methods. Single nucleotide resolution of poly(A) species in the 100−150 nt range is achievable by capillary gel electrophoresis,[26,27] but requires a viscous high molecular weight gel matrices. Chromatographic techniques of ion-exchange (IEX) and ion-pair reversed-phase (IP RP) LC are methods of choice for separation of short oligonucleotides,[28−32] including antisense oligonucleotides (ASO) and silencing RNA (siRNA). The separation of $n/n - x$ oligonucleotides, where x is the number of truncated nucleotides, is readily achievable for oligonucleotides up to 25 nucleotides long. A limited number of reports describe LC separation of >50 nt oligonucleotides,[31,33] while >100 nt species are extremely difficult to analyze with $n/n - 1$ resolution.[28,34] Separations of >100 nt single-stranded (ss) and double-stranded (ds) nucleic acids are described in the literature with IEX and IP RP LC; however, the resolution decreases with the nucleic acid length and does not afford $n/n - 1$ resolution.[12,13,35,36]

Size exclusion chromatography (SEC) is a method that separates the compounds according to their size.[37] The technique is widely used for the analysis or purification of polymers and proteins.[38] SEC was, to a lesser extent, applied to the separation of oligonucleotides and nucleic acids.[39−43] This may be because the SEC technique has a relatively low separation power compared to IEX or RP LC or electromigration methods used for nucleic acids analysis.[12,26,28,30,31,33,44−46] Nevertheless, SEC has been shown to be a robust and powerful method for RNA purification,[40,42] therapeutic oligonucleotide analysis,[41] and elucidation of the oligonucleotide secondary structure.[43] Because of SEC simplicity and availability of SEC columns with an improved resolution, the SEC technique can become a useful tool for the analysis of therapeutic oligonucleotides and mRNA.

In this work, we focused on the characterization of the poly(A) tail of mRNA. Our goal was to develop chromatographic methods for the analysis of the length and heterogeneity of the 100−150 nt long poly(A) tail after its cleavage from the intact mRNA molecule. The results of the developed SEC and IP RP LC methods with easy-to-implement UV detection were confirmed by the LC MS method.

EXPERIMENTAL SECTION

Materials and Chemicals. CleanCap EPO mRNA 1 mg/mL (EPO mRNA) was purchased from TriLink Biotechnologies, San Diego, CA, USA. FLuc-beta mRNA (FlucB mRNA) 1.6 mg/mL was obtained from AmpTech, Hamburg, Germany. Optima LC MS grade acetonitrile, RNase T1 endoribonuclease, and PES 500 mL 0.1 μm filters were purchased from Thermo-Fisher Scientific, Waltham, MA USA. The enzymatic reaction was performed in 0.2 mL individual domed PCR tubes using a T100 thermal cycler (both Bio-Rad laboratories, Hercules, CA, USA) set to 37 °C. Deionized water was produced using a Milli-Q system, Millipore, St. Louis, MO, USA. Glacial acetic acid (AA), octylamine (OA; > 99.5%), sodium phosphate monobasic, sodium phosphate dibasic, 1 M solution of triethylammonium acetate (TEAA), and RNase-free water, 1,1,1,3,3,3-Hexafluoro-2-propanol (HFIP, > 99.5%) were purchased from Sigma-Aldrich, St. Louis, MO, USA. Oligodeoxyribonucleotides with adenosine (dA_n) and thymidine (dT_n) sequences and oligoribonucleotides with the adenosine sequence (rA_n, custom synthesis) were purchased from Integrated DNA Technologies (Coralville, IA, USA). All synthetic oligonucleotides were used desalted but unpurified. 10× rCutSmart buffer and Quick CIP enzyme were purchased from New England Biolabs (Ipswich, MA, USA). The μElution Oasis HLB 96-well solid phase extraction (SPE; 2 mg sorbent/well) plate and 96-well sample collection plates (polypropylene 350 μL) were obtained from Waters Corporation (Milford, MA, USA). An Allegra X-14 centrifuge equipped with a SX4750A rotor (Beckman Coulter, Brea, CA, USA) was used for SPE sample cleanup.

LC UV and LC MS Instrument Columns and Conditions. SEC and IP RP LC UV experiments were performed using an ACQUITY UPLC H-Class premier system with an ACQUITY photodiode array detector equipped with a Titanium 5 mm detector cell (Waters Corporation, Milford, MA, USA). The SEC analysis of poly(A) tail analysis was performed with the ACQUITY premier protein SEC column, 250 Å, 1.7 μm, 4.6 × 150 mm, obtained from Waters Corporation, Milford, MA, USA. SEC method development was also performed with the 1.7 μm, 4.6 × 150 mm ACQUITY protein SEC column, 125 Å, and 2.5 μm, 4.6 × 150 mm ACQUITY protein SEC column, 450 Å. (Waters Corporation, Milford, MA, USA). The SEC mobile phase consisted of aqueous 0.1 M phosphate buffer, pH 8. The mobile phase was prepared by dissolving 6.72 g of Na_2HPO_4 and 0.32 g of NaH_2PO_4 in 500 mL of deionized Milli-Q water. The SEC mobile phase was sterilized by filtering the solution with a PES 500 mL 0.1 μm filter. The SEC separation was performed at a flow rate of 0.2 mL/min at 25 °C; the UV detection wavelength was 260 nm.

IP RP LC experiments were performed with the same ACQUITY UPLC H-Class premier system as described above. The separation column was an ACQUITY premier oligonucleotide BEH C18 column, 300 Å, 1.7 μm, 2.1 × 150 mm (Waters Corporation, Milford, MA, USA). Mobile phase A was 0.1 M octylammonium acetate (OAA) buffer in 40% acetonitrile and 1% HFIP (mix 116.13 g of deionized water with 60.86 g of acetonitrile; add 1.145 mL of glacial acetic acid, 3.305 mL of octylamine, and 2 mL of HFIP). Mobile phase B was 0.1 M OAA buffer in 90% acetonitrile and 1% HFIP (mix

https://doi.org/10.1021/acs.analchem.3c02552
Anal. Chem. 2023, 95, 14308−14316

19.36 g of deionized water with 136.92 g of acetonitrile; add 1.145 mL of glacial acetic acid, 3.305 mL of octylamine, and 2 mL of HFIP). The mobile phases A and B contained acetonitrile to improve the solubility of hydrophobic OA. The rationale for including HFIP (pK_a 9.3) was to maintain the mobile phase pH in the mild basic range and mitigate pH shifts in the case of minor OA (pK_a 10.7) and acetic acid (pK_a 4.8) pipetting errors. Without addition of HFIP, the buffer pH can fluctuate in the range of several pH units. Because of the high concentration of ion-pairing buffer, the inclusion of HFIP does not make the mobile phase compatible with MS detection.[34] Mobile phase D was pure acetonitrile. The flow rate was 0.3 mL/min, column temperature was 60 °C, and UV detection wavelength was 260 nm. Mobile phase gradient was from 46% A and 54% B to 28% A, 62% B, and 10% D in 40 min. The column was then washed with pure acetonitrile mobile phase D for 1 min and equilibrated at initial gradient conditions for 15 min.

IP RP LC MS poly(A) analysis experiment was performed with a BioAccord LC MS system equipped with the ACQUITY Premier UPLC H-Class Premier system. The separation column was the ACQUITY Premier Oligonucleotide C18, 130 Å, 1.7 μm, 50 × 2.1 mm column protected by a VanGuard Premier FIT 1.7 μm, 5 × 2.1 mm cartridge (all Waters Corporation, Milford, MA, USA). The flow rate was 0.3 mL/min, column temperature is 60 °C, and UV detection wavelength is 260 nm. Mobile phase A was 8 mM N,N-diisopropyl-ethylamine (DIPEA) and 40 mM HFIP in deionized water, pH 8.8. Mobile phase B consisted of 4 mM DIPEA and 4 mM HFIP in 75% ethanol. DIPEA/HFIP is a suitable ion-pairing system for sensitive LC MS analysis.[47,48] The gradient was from 25 to 40% B in 10 min followed by 1 min wash with 85% B and 4 min equilibration at initial gradient conditions. The MS instrument was operated in negative mode, 400−5000 Da mass range, cone voltage 45 V, and 1 s MS scan.

The LC UV and LC MS data were acquired with Empower v 3.0 and MassLynx 4.2 Software, respectively. MS data deconvolution was performed with MaxEnt1 software (all Waters Corporation, Milford, MA, USA).

mRNA Digestion. EPO mRNA or FlucB mRNA samples were digested with RNase T1 using the following protocol: 10 μL of the mRNA solution was mixed with 28 μL of RNase-free water and 4 μL of 10× CutSmart buffer. 1.5 μL (1.5 units) of RNase T1 enzyme was mixed with the sample, and the cleavage reaction was carried out for 30−60 min at 37 °C. After mRNA digestion, the sample was spiked with 0.2 μL (1 unit) of Quick CIP enzyme to remove residual phosphate from the 5′ or 3′ end of the oligonucleotides. The addition of the Quick CIP enzyme was not necessary, but it improved the solution stability of the poly(A) cleaved product and synthetic oligonucleotide standards by eliminating minor (phosphorylated) peaks from SEC and IP RP LC analyses. After 20 min of Quick CIP dephosphorylation at 37 °C, the sample was transferred into a glass vial and kept in the LC instrument sample manager at 10 °C prior to analysis. Typically, 2 μL was injected for SEC. The sample was purified prior to IP RP LC analysis using a solid phase extraction (SPE) plate as described in the following section. The SPE sample purification extended the lifetime of the RP LC column.

mRNA RNase T1 Digest Sample Preparation. The RNase T1-digested mRNA sample was purified using an μElution Oasis HLB 96-well SPE plate. The sample, wash, and elution fractions were passed through the sorbent bed by centrifugation (30−180 s at 1000 g). The liquid fractions were collected into a 96-well collection plate stacked under the SPE plate. The selected SPE wells were first washed with 50 μL of acetonitrile and then equilibrated with 100 μL of 0.1 M TEAA solution. The digested mRNA sample (43.7 μL) was mixed with 4 μL of 1 M TEAA and two vials of the digest; that is, 95.4 μL was loaded on the SPE plate. The solution was collected in a clean collection plate and reloaded for the second time onto the same SPE well to reduce potential sample breakthrough.[45] The loaded SPE well was washed with 30 μL of 0.1 M TEAA and then eluted with 40 μL of 30% acetonitrile. The eluent was collected in a clean collection plate, transferred into a glass HPLC vial, and placed in the LC sample manager set to 10 °C. Ten μL of the sample was injected on the column for IP RP LC analysis.

RESULTS

Size Exclusion Method Development for Poly(A) Tail Length Analysis. In size exclusion chromatography, the analytes are separated according to their ability to penetrate the chromatographic sorbent pores. Smaller molecules are more retained than larger molecules, which are partially excluded from the pore volume. The molecular size range of analytes separated in SEC depends on the sorbent pore size. We used three SEC columns with different pore sizes to investigate the resolution of oligonucleotides and SEC calibration linearity. Figure 1 shows the separation of 5, 10, 15, 20, 30, 40, 50, 60, 80, 100, 120, and 150 nt oligodeoxyribonucleotide adenosine mixtures (we will refer to this sample as dA_{5-150}). Minor peaks present in the sample

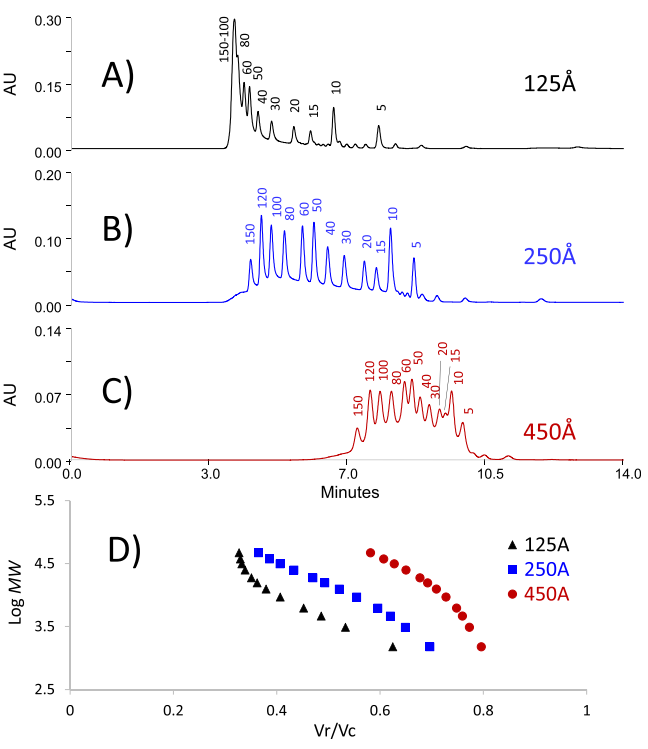

Figure 1. SEC separation of dA_{5-150} oligonucleotides using columns packed with 125 Å (A), 250 Å (B), and 450 Å (C) pore size sorbent. Panel (D) plots the experimental data as SEC calibration curves. 250 Å column has linear calibration for the 30−150 nt oligonucleotide range (see Figure 2A).

https://doi.org/10.1021/acs.analchem.3c02552
Anal. Chem. 2023, 95, 14308−14316

are failed synthesis products or failure sequences. Because the oligo(A) species do not have a strong secondary structure, the analysis was performed at 25 °C. The flow rate 0.2 mL/min was selected as a compromise between the optimal flow rate (<0.2 mL/min)[49] and speed of analysis. We selected 0.1 M phosphate buffer, pH 8, as the mobile phase to minimize the potential nonspecific adsorption of nucleic acid to the column hardware.[50−52] Figure 1A shows that the 125 Å SEC column is more suitable for separation of short oligonucleotides; the $n/n-1$ resolution was observed for dA_n species up to 15 nt long oligonucleotides (see minor peaks in Figure 1A). On the other hand, the longer oligonucleotides (80−150 nt) are not resolved with the 125 Å SEC column; they elute as a single peak near the pore exclusion limit of the sorbent. The 250 Å SEC column appears to be a good choice for separation of the dA_{5-150} sample; separation of short oligonucleotides is partially lost, but longer oligonucleotides are clearly resolved (Figure 1B). The third experiment with the 450 Å SEC column (Figure 1C) shows that this column is suitable for separation of >150 nt oligonucleotides, while the resolution of <60 nt species is inferior compared to 125 and 250 Å SEC columns. The chromatographic data in Figure 1A−C were used to construct traditional SEC calibration plots presented in Figure 1D. The x-axis plots the oligonucleotide elution volume V_r ($V_r = t_r \times F$; t_r is retention time and F is flow rate) normalized to empty column ($V_c = \pi \times d^2/4 \times L$; d is column internal diameter and L is column length), while the y-axis is the logarithmic value of analyte molecular weight (log MW). The useful SEC separation region is near the center, where the calibration plot is linear. In the regions where the plot bends upward or downward, the analyte size approaches either the exclusion limit of the sorbent pores ($V_r/V_c \sim 0.3$; bulky analytes elute in the interstitial volume between the sorbent particles) or the full inclusion limit of the sorbent pores ($V_r/V_c \sim 0.8$; small analytes enter all pores unrestricted and elute in the column void volume). In both extreme cases, the SEC resolution is lost for the given class of analytes. This could be seen for calibration plots of the 125 Å SEC column for >80 nt oligonucleotides and for the 450 Å SEC plot for <10 nt oligonucleotides (Figure 1D). The 250 Å SEC columns provided the best separation of the 30−150 nt oligonucleotides. Therefore, we selected this column for poly(A) tail analysis within this corresponding range.

SEC Calibration for RNA Poly(A) Tail Measurement. We evaluated the linearity of 250 Å SEC columns with the adenosine dA_{5-150} standard. For simplicity, the calibration curve was directly plotted as a function of retention time versus log N (N is the number of nucleotides). The calibration curve was linear for the dA_n range 30−150 nt with a coefficient of determination $R^2 \sim 0.999$ (Figure 2A). This means that the length of the dA_n oligonucleotides can be accurately measured from their SEC retention time. The choice of dA_n oligonucleotides for SEC calibration was motivated by their easy availability. Synthetic dA_n oligonucleotides are relatively inexpensive and can be purchased from vendors in high quality up to 150 nt in length. However, further experiments reveal that dA_n has somewhat different retention in SEC compared to oligodeoxythymidine (dT_n) standards, and an even greater retention difference was observed for oligoribonucleotide adenosines rA_n (chromatograms in Figure 2B, C, and D, respectively; the dashed lines were added for retention shift visualization). This behavior is likely related to different hydrodynamic sizes of oligonucleotide samples rather than due

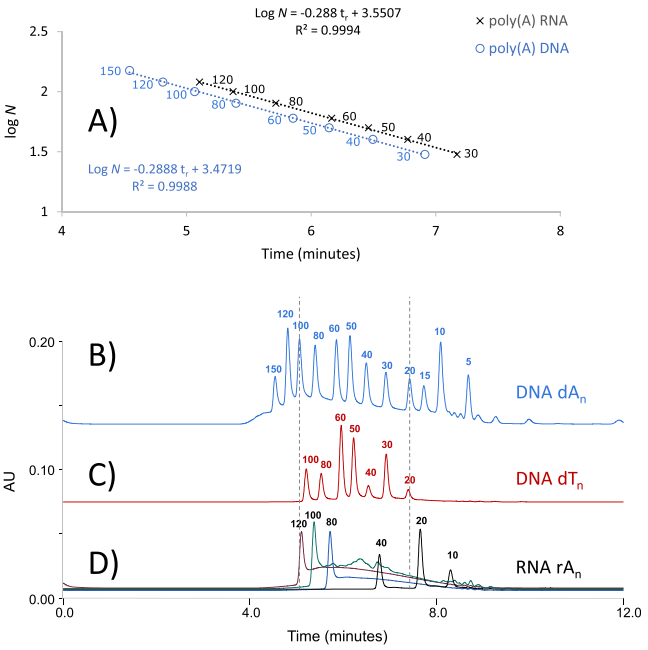

Figure 2. Panel (A) compares SEC calibrations obtained for RNA (rA_{5-120}) and DNA (rA_{5-150}) oligonucleotides. SEC chromatograms of dA_{5-150}, dT_{20-100}, and rA_{10-120} synthetic oligonucleotide standards are shown in panels (B), (C), and (D), respectively. Dotted lines highlight the observed differences in the oligonucleotide SEC retention. Data were acquired with an ACQUITY Premier Protein SEC column, 250 Å, 1.7 μm, 4.6 × 150 mm.

to the ionic or hydrophobic interactions of oligonucleotides with the SEC sorbent. Addition of 10−20% of methanol to the mobile phase or change of buffer concentration did not alter the relative retention of dA_n, dT_n, and rA_n standards. Because of the retention shift of different types of oligonucleotides, we purchased rA_n standards chemically consistent with the poly(A) RNA tail and prepared oligoribonucleotide(A) calibration (Figure 2A) that can be directly used for poly(A) RNA tail length SEC measurement.

SEC Poly(A) Tail Length Measurement. FLuc-beta and EPO mRNA samples obtained from vendors were used for poly(A) tail length measurement by the SEC method. The mRNA samples were digested with RNase T1 as described in the Materials and Methods section. RNase H or other nucleases can also be used to liberate the poly(A) tail from mRNA.[15,18] The advantage of RNase T1 is its high specificity compared to other enzymes.[18,22,25] RNase T1 nuclease cleaves single-stranded RNA sequences at G/N motifs, producing numerous short oligonucleotides suitable for mRNA or sgRNA mapping.[15,25] Since the poly(A) tail portion of mRNA does not contain G nucleotides, the 3′ poly(A) tail is cleaved from mRNA as a sizable 100−150 nt oligonucleotide, which significantly exceeds in length the remaining products of RNase T1 cleavage (1−30 nt species). Consequently, the poly(A) tail can be separated using an earlier described SEC method based on the 250 Å sorbent. The example of poly(A) tail SEC analysis of FLuc-beta mRNA is shown in Figure 3. The red chromatogram represents the peak of the intact FLuc-beta mRNA molecule prior to RNase T1 digestion (1970 nt long including the 120 nt poly(A) tail). The blue chromatogram represents the SEC analysis after the FLuc-beta mRNA digestion yielding 2−30 nt oligonucleotides and a 3′ poly(A) tail peak at t_r = 5.007 min. For illustration, we overlaid the

https://doi.org/10.1021/acs.analchem.3c02552
Anal. Chem. 2023, 95, 14308−14316

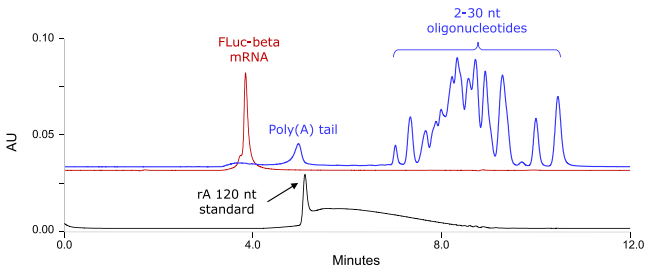

Figure 3. SEC analysis of intact FLuc-beta mRNA (1970 nt, red chromatogram) and FLuc-beta mRNA digested with RNase T1 (blue chromatogram; the peak eluting near 5 min represents poly(A) tail signal). Black chromatogram is SEC analysis of the rA_{120} oligonucleotide; the standard is contaminated with truncated synthetic impurities eluting within a peak tail.

results with the injection of the rA_{120} synthetic oligonucleotide (black chromatogram). The 120 nt standard (containing a long tail of shorter synthetic impurities) elutes closely after the poly(A) tail peak. This suggests that the poly(A) tail is longer than the 120 nt. For more accurate estimation of the poly(A) tail length, we used the calibration curve $\log N = -0.288 \times t_r + 3.5507$ presented in Figure 2. The experimentally measured retention time 5.007 min yields the poly(A) tail length of 128 nt. The analysis of the second EPO mRNA sample showed a poly(A) tail peak at 5.061 min, which gives a poly(A) tail length of 123 nt (for chromatogram see Figure S1).

Closer inspection of Figure 3 shows that the poly(A) tail peak is noticeably wider than the peak of the rA_{120} synthetic standard.

This is likely due to the heterogeneity of the poly(A) tail formed during the polyadenylation of mRNA. In other words, the calculated 128 nt length of poly(A) is only an average length of the multiple poly(A) tail species coeluting as a single peak because the SEC method does not have the resolution power to separate these closely related oligonucleotides. The peak broadening is a manifestation of a partial separation of the poly(A) tail species present in the sample. The investigation of heterogeneity of poly(A) tail length requires high-resolution chromatography or the MS method. The development of such a method is described in the next section.

IP RP LC Method Optimization for Separation of 100−150 nt Oligonucleotides. IP RP LC is a high-resolution method capable of $n/n-1$ separation of 60 nt and potentially even longer oligonucleotides.[31,33] Gilar et al. outlined strategies for improving the oligonucleotide separation in IP RP LC; the recommendations include use of efficient columns packed with 2.5 or 1.7 μm UPLC particles,[32] shallow gradients,[53] and optimized ion-pairing mobile phases.[54] Recently, Donegan et al.[34] demonstrated that hydrophobic ion-pairing reagents such as OAA facilitate an improved oligonucleotide separation relative to hydrophilic ion-pairing systems. Based on these guidelines, we selected an efficient 150 × 2.1 mm column packed with 1.7 μm 300 Å C_{18} sorbent, shallow gradient, and a hydrophobic OAA ion-pairing mobile phase system. According to reports,[34,54] the oligonucleotide resolution improves with ion-pairing buffer concentration. We evaluated 50−110 mM of OAA systems and observed the corresponding improvements in resolution (data not shown). However, high concentrations of OAA led to high oligonucleotide retention and required >80% acetonitrile for elution at which point we observed the loss of signal for >120 nt oligonucleotides presumably due to sample precipitation on the column. Therefore, we limited the OAA concentration to 100 mM in mobile phase A and B (containing 40 and 90% acetonitrile, respectively) and employed a gradient of mobile phase D containing 100% acetonitrile. In the optimized method, the gradient started at 46% A, 54% B, and 0% D and concluded at 28% A, 62% B, and 10% D in 40 min. Expressed in percentage of acetonitrile, the gradient was 67% to 77% of acetonitrile in 40 min (0.25% acetonitrile/min); in terms of ion-pairing concentration, the gradient started at 100 mM and finished at 90 mM OAA in 40 min. The chosen mobile phase was optimized for oligonucleotide LC separation, but it is not compatible with MS. Two-dimensional LC could be implemented when the MS detection is desired.[55,56]

IP RP LC Study of Poly(A) Heterogeneity. The mRNA poly(A) tail sample prepared according to Materials and Methods (mRNA was digested with RNase T1 and purified by SPE) was analyzed by the IP RP LC method; the chromatograms are presented in Figure 4. Short RNA oligonucleotides

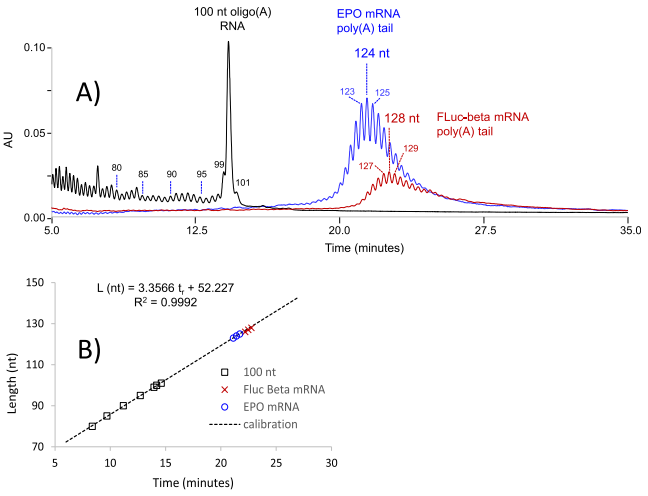

Figure 4. (A) IP RP LC analysis of the poly(A)tail released from EPO mRNA (blue chromatogram) and the FLuc-beta mRNA sample (red chromatogram) with RNase T1. IP RP LC analysis of the rA_{100} standard and its truncated oligonucleotides is shown as a black chromatogram. The retention data of 80, 85, 90, 95, 99, 100, and 101 nt rA_n oligonucleotides were plotted as a calibration curve (panel B) and utilized to estimate the mRNA poly(A) tail species length. For additional data, see Figure S3.

were eluted before 5 min (data not shown, UV signal exceeded 1 AU), while the poly(A) tail species eluted approximately between 20 and 25 min. EPO mRNA (blue chromatogram) and FLuc-beta mRNA (red chromatogram) analyses reveal the presence of heterogeneous poly(A) tail species consisting of 5−10 dominant peaks and many minor species. The IP RP LC method does not provide a baseline separation, but the peak resolution is sufficient to visualize and quantify the poly(A) tail heterogeneity.

Poly(A) tail chromatograms in Figure 4 are overlaid with the synthetic rA_{100} oligonucleotide (black trace). The 100 nt oligoadenosine contains a ladder of synthetic n-x impurities eluting prior to the main peak. These impurities were utilized to plot the relationship between the length of the rA_n species and the retention time. This plot appears to be linear (Figure 4 inset) and could be used to extrapolate the mRNA poly(A)tail species length. According to this calibration, the prominent poly(A) tail species labeled in Figure 4 were 124 nt for EPO

https://doi.org/10.1021/acs.analchem.3c02552
Anal. Chem. 2023, 95, 14308−14316

mRNA and 128 nt for the FLuc-beta mRNA sample. These results are consistent with the poly(A) tail length measurement performed with the SEC method described in the previous section. Additional calibration with rA_{100} and rA_{120} synthetic standards (Figure S2) or standards directly spiked to EPO and FLuc-beta mRNA digests (Figure S3) confirmed our measurement. The data could not be directly confirmed with MS because the mobile phases of both SEC and IP RP LC methods were not compatible with mass spectrometry analysis.

IP RP LC MS Analysis of Poly(A) Tail. The poly(A) tail length was investigated also with the IP RP LC-MS method with mobile phases consisting of DIPEA/HFIP aqueous buffer. This mobile phase is well suited for sensitive LC-MS analysis of oligonucleotides.[47,48] The IP RP LC mobile phases where the alkylamines are buffered by HFIP instead of acetic acid provide a significantly greater MS signal for oligonucleotide analysis.[34,57] The RNase T1-digested FLuc-beta mRNA sample was eluted from the chromatographic column with a fast 10 min gradient. Figure 5 shows the resulting chromatogram.

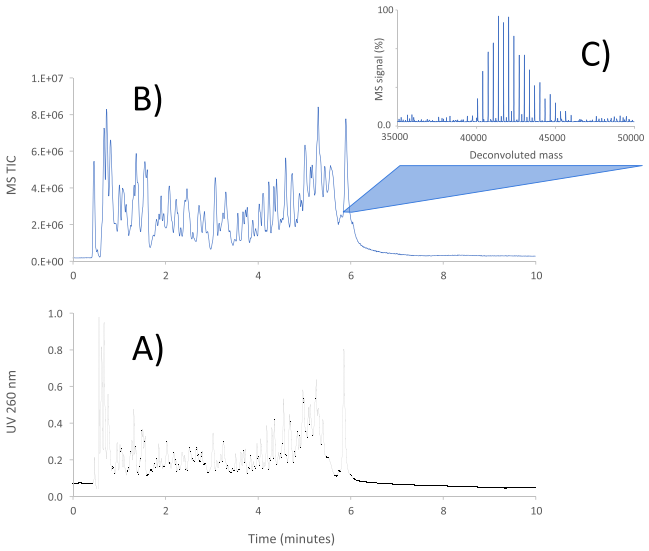

Figure 5. IP RP LC analysis of FLuc-beta mRNA poly(A) tail. (A) LC UV analysis, (B) LC MS LC MS total ion chromatogram (TIC), and (C) deconvolved ESI-MS spectrum of the peak eluting close to 6 min. This chromatographic peak corresponds to a mixture of heterogeneous poly(A) species with three most dominant MS signals corresponding to 126, 127, and 128 nt oligonucleotides.

Short RNA oligonucleotides elute before the last distinct peak at 6 min, presumably the poly(A) tail signal. The MS signal under this peak was summed, and the multiply charged MS ions were deconvoluted with MaxEnt1 software into zero charge MS spectrum presented as Figure 5C. The three most dominant MS signals in the spectrum correspond to 126, 127, and 128 nt long poly(A) species. This result is consistent with previously obtained results from SEC and IP RP LC UV analysis.

DISCUSSION

SEC is used in the industry mainly for analysis of synthetic polymers and proteins, and it is applicable to analysis of RNA/DNA therapeutics as well. In the initial experiment, we investigated the selection of the SEC sorbent pore size for targeted separation of poly(A) tail species from shorter oligonucleotides and intact mRNA. This evaluation was essential since the SEC sorbent pore size selection suitable for separation of the target oligonucleotide length is not well-known. Kim and colleagues[42] reported that the molecular weight range of proteins separable in SEC does not directly translate to oligonucleotides. This is because linear nucleic acids have a larger hydrodynamic radius than globular proteins. We confirmed this observation in experiments with the 250 Å SEC column (Figure S4). Indeed, large differences in log MW = $a \times t_r + b$ calibrations were found between oligonucleotides and protein standards.

The sequence or secondary structure (stems, loops, duplexes, and structural polymorphisms) also has an impact on SEC retention of oligonucleotides.[43] This can be seen in the chromatograms shown in Figure 2B–D for dA_n, dT_n, and rA_n samples. Even though the used homooligomeric samples do not have a strong secondary structure, their retention is not the same. We investigated whether the differences are due to secondary ionic or hydrophobic interactions of analytes with the SEC sorbent. Neither the addition of methanol (10 or 20%) nor the change in the buffer type and concentration yielded the retention strictly according to the oligonucleotide length. We concluded that retention differences were most likely a manifestation of the different oligonucleotide hydrodynamic sizes. This unfortunately means that it is necessary to use expensive rA_n standards as calibrants for poly(A) tail RNA measurement instead of more affordable dA_n, as we originally planned. This problem with calibration standards could be circumvented, as illustrated in Figure 2A. Two linear calibrations were constructed for the same column using dA_n and rA_n standards. The calibrations have essentially the same slope with a small difference in the intercept. This, in principle, means that a retention time correction factor can be applied to superimpose the dA_n calibration onto the rA_n calibration curve (see Figure S5). The concept of using dA_n standards as surrogates for rA_n calibrants in SEC was validated with two UPLC systems and three SEC columns. The experiments confirmed that the dA_n and rA_n calibrations are parallel. When the correction factor Δt_r = 0.306 min is used to adjust experimental dA_n retention times, both dA_n and rA_n SEC calibration curves become virtually identical (Figure S5B). Table S1 lists the retention data of four SEC experiments with dA_n and rA_n calibrants. The average retention difference between rA_n and dA_n represents the proposed correction factor Δt_r of 0.306 min. While the tubing volume and injection loop size of LC instrument affect the absolute retention times of calibrants in SEC, the relative retention difference between rA_n and dA_n standards remains constant (Table S1). Therefore, it is possible to utilize inexpensive, readily available, and chemically stable dA_n oligonucleotides as surrogates for the rA_n calibration standards. In the simplest implementation, the analyst can add the Δt_r = 0.306 min correction factor to the measured dA_n retention times (Figure S5) prior to plotting the calibration curve log $N = a \times t_r + b$. The resulting SEC calibration is directly applicable for mRNA poly(A) tail measurement.

We investigated the comparability of rA_n and dA_n calibrations for poly(A) tail analysis of EPO and Fluc-beta mRNA samples. Table S2 lists the retention data of four experiments and their interpretation using rA_n and corrected dA_n SEC calibrations (using a 0.306 min correction factor). Both calibrations gave similar poly(A) tail length measurement within one nucleotide length difference for calibrations obtained with 40–120 nt standards. When we used 40–150

https://doi.org/10.1021/acs.analchem.3c02552
Anal. Chem. 2023, 95, 14308−14316

nt dA_n calibration standards, the calculated length of the poly(A) tail was approximately 3 nt longer. This is due to the change in the calibration slope caused by the 150 nt data point deviating slightly from the linear trend. 150 nt dA standard appears to lie at the upper range of the calibration linearity (Figures 2A and S5B).

The 250 Å column chosen for SEC analysis has metal hardware modified with ethylene-bridged siloxane-modified metal surface chemistry known as hybrid surface technology (HST).[50,58] HST has been shown to mitigate the nonspecific adsorption of nucleic acid on LC hardware, which can have an adverse effect on oligonucleotide analysis.[51,52,59] The 100 mM phosphate buffer and basic pH were shown to reduce the nonspecific adsorption,[50] but HST columns are preferred for nucleic acid analysis when available.

The IP RP LC method is a high-resolution method capable of simultaneously measuring poly(A) tail length and heterogeneity, which makes the SEC method seemingly redundant. However, IP RP LC is significantly more complex and less robust than the isocratic SEC method.[60] The method described in this work is optimized for the separation of 100−150 nt poly(A) tail oligonucleotides. In IP RP LC, a small drift of retention times is sometimes detected.[61] This is due to the evaporation of semivolatile ion-pairing mobile phases, incomplete thermal equilibration of the column, and inconsistent column equilibration time between injections. Such a retention shift can affect the poly(A) length measurement accuracy. Calibration with size standards should be performed prior or after the sample analysis (Figure 4) or the rA_n standards can be spiked to the sample as shown in Figure S3.

RNase T1 utilized in this work cleaves mRNA at the G/N motifs. Due to cleavage selectivity, the liberated poly(A) tail sequence may contain one or several additional nucleotides at the 5′ end other than G. The sequence of interrogated mRNA is typically known; this knowledge should be utilized in the poly(A) tail length measurement as was the case with FLuc-beta mRNA analysis in this study. The poly(A) tail fragment created with RNase T1 cleavage contained a single additional cytidine at the 5′ end (see Figure S6). The poly(A) analysis of the second sample, EPO mRNA, is complicated by the fact that the full sequence of EPO mRNA was not provided by the manufacturer. The exact number of additional nucleotides at the 5′ end of the EPO mRNA poly(A) tail after RNase T1 cleavage is not known. The length of the EPO mRNA poly(A) tail reported in Figures S1 and S3 (123 nt) should be treated as an approximation. This result was consistent with EPO mRNA poly(A) LC MS measurement (Figure S7).

We should also mention that the applicability of RNase T1 for digestion of BioNTech/Pfizer SARS-Cov-2 mRNA vaccine is complicated by the fact that the poly(A) tail includes a 10 nt long motif including G nucleotides. In this case, RNase T1 will generate two sections of the poly(A) tail (Figure S8). The mRNA sequence should be always consulted prior to measurement; other enzymes can be used for mRNA poly(A) tail cleavage if desired.[15,17,18,22,23]

CONCLUSIONS

We demonstrate that the SEC column with 250 Å pore size is suitable for the separation of 40−150 nt long oligonucleotides with log N vs t_r calibration linearity. The developed method was applied to robust and repeatable measurement of the poly(A) tail length after its cleavage form mRNA. Because synthetic poly(A) RNA standards are scarce, we evaluated the utility of oligo(A) DNA surrogate standards for SEC calibration. After we applied an experimentally derived retention correction, the surrogate SEC standard calibration provided virtually identical poly(A) tail measurement results as those of RNA poly(A) tail calibrants (Tables S1 and S2).

The SEC method provides information about an average poly(A) tail length, but it cannot directly measure the microheterogeneity of the mRNA 3′-end. The microheterogeneity analysis of the poly(A) tail was performed with a high-resolution IP RP LC method based on the OAA ion-pairing system. This method can resolve poly(A) tail species differing in a single nucleotide up to approximately 150 nt in length. SEC and IP RP LC methods use simple UV detection, which makes them suitable for routine quality control of mRNA analysis.

The performance of the SEC and IP RP LC methods for poly(A) tail characterization was verified with LC-MS (Figures 5, S7, and S9). The LC-MS method resolves short RNA oligonucleotides RNase T1 digestion products from poly(A) tail in a 10 min gradient using the MS compatible mobile phase. The summed and deconvoluted MS data of the poly(A) tail peak (Figures 5C, S7, and S9) reveal dominant MS signals corresponding to 126, 127, and 128 nt long oligonucleotides for the Fluc-beta mRNA sample (125−127 nt long rA_n sequences plus one cytidine) and 122−124 nt long oligonucleotides for the EPO mRNA sample. The LC-MS results are consistent with IP RP LC UV and SEC UV measurements presented in Figures 3, S1, and S3. This finding confirms that the developed SEC and IP R P LC methods for poly(A) tail length measurement provide accurate and useful results and are applicable to mRNA quality control. The LC-MS method utilized more expensive high-resolution MS instrument and deconvolution software, but it provides data-rich results, including the direct molecular weight measurement of poly(A) tail species and the molecular weight difference between the observed poly(A) species (329.2 Da mass differences in the MS spectrum presented in Figure 5C confirm that the microheterogeneity is due to different numbers of A mononucleotides in the poly(A) tail). We expect that LC MS will be a preferred method for mRNA analysis in biopharma research.

ASSOCIATED CONTENT

Supporting Information

The Supporting Information is available free of charge at https://pubs.acs.org/doi/10.1021/acs.analchem.3c02552.

Chromatograms, IP RP LC calibration curve, SEC calibration curve, mass spectrometry spectra, and sequences of mRNA (PDF)

AUTHOR INFORMATION

Corresponding Author

Martin Gilar − *Separations R&D, Waters Corporation, Milford, Massachusetts 01757, United States;* orcid.org/0000-0003-1199-1287; Email: martin_gilar@waters.com

Authors

Catalin Doneanu − *Discovery and Development, Waters Corporation, Milford, Massachusetts 01757, United States*

Maissa M. Gaye − *Consumables Research, Waters Corporation, Milford, Massachusetts 01757, United States*

https://doi.org/10.1021/acs.analchem.3c02552
Anal. Chem. 2023, 95, 14308−14316

Complete contact information is available at:
https://pubs.acs.org/10.1021/acs.analchem.3c02552

Author Contributions

The manuscript was written through contributions of all authors. All authors have given approval to the final version of the manuscript.

Notes

The authors declare the following competing financial interest(s): The authors are employee of Waters Corporation, manufacturer of some consumables and instruments used in this study.

ACQUITY, UPLC, BEH, Empower, MassLynx, BioAccord, VanGuard, and Oasis are trademarks of Waters Technologies Corporation. CleanCap is a trademark of TriLink BioTechnologies, LCC. rCutSmart is a trademark of New England Biolabs. Mill-Q is a trademark of Merck KGaA.

■ ACKNOWLEDGMENTS

We thank Matthew Lauber and Joseph Fredette for their comments to the manuscript.

■ REFERENCES

(1) Castells, M. C.; Phillips, E. J. *N. Engl. J. Med.* **2021**, *384* (7), 643−649.
(2) Gote, V.; Bolla, P. K.; Kommineni, N.; Butreddy, A.; Nukala, P. K.; Palakurthi, S. S.; Khan, W. *Int. J. Mol. Sci.* **2023**, *24* (3), 2700.
(3) Watanabe, A.; Kani, R.; Iwagami, M.; Takagi, H.; Yasuhara, J.; Kuno, T. *JAMA Pediatr.* **2023**, *177* (4), 384−394.
(4) Chaudhary, N.; Weissman, D.; Whitehead, K. A. *Nat. Rev. Drug Discovery* **2021**, *20* (11), 817−838.
(5) Magadum, A.; Kaur, K.; Zangi, L. *Mol. Ther.* **2019**, *27* (4), 785−793.
(6) Miao, L.; Zhang, Y.; Huang, L. *Mol. Cancer* **2021**, *20* (1), 41.
(7) Lorentzen, C. L.; Haanen, J. B.; Met, Ö.; Svane, I. M. *Lancet Oncol.* **2022**, *23* (10), e450−e458.
(8) Weide, B.; Carralot, J. P.; Reese, A.; Scheel, B.; Eigentler, T. K.; Hoerr, I.; Rammensee, H. G.; Garbe, C.; Pascolo, S. *J. Immunother.* **2008**, *31* (2), 180−188.
(9) Curreri, A.; Sankholkar, D.; Mitragotri, S.; Zhao, Z. *Bioeng. Transl. Med.* **2023**, *8* (1), No. e10374.
(10) USP, Analytical Procedures for mRNA Vaccine Quality, 2nd draft. *USP Draft Guidelines* **2023**, EA966W_2022−03.
(11) Bloom, K.; van den Berg, F.; Arbuthnot, P. *Gene Ther.* **2021**, *28* (3−4), 117−129.
(12) Kanavarioti, A. *Sci. Rep.* **2019**, *9* (1), 1019.
(13) Fekete, S.; Yang, H.; Wyndham, K.; Lauber, M. *J. Chromatogr. Open* **2022**, *2*, No. 100031.
(14) Packer, M.; Gyawali, D.; Yerabolu, R.; Schariter, J.; White, P. *Nat. Commun.* **2021**, *12* (1), 6777.
(15) Jiang, T.; Yu, N.; Kim, J.; Murgo, J. R.; Kissai, M.; Ravichandran, K.; Miracco, E. J.; Presnyak, V.; Hua, S. *Anal. Chem.* **2019**, *91* (13), 8500−8506.
(16) Wolf, E. J.; Grünberg, S.; Dai, N.; Chen, T. H.; Roy, B.; Yigit, E.; Corrêa, I. R. *Nucleic Acids Res.* **2022**, *50* (18), No. e106.
(17) Nwokeoji, A. O.; Earll, M. E.; Kilby, P. M.; Portwood, D. E.; Dickman, M. J. *J. Chromatogr. B Analyt. Technol. Biomed. Life Sci.* **2019**, *1104*, 212−219.
(18) Beverly, M.; Dell, A.; Parmar, P.; Houghton, L. *Anal. Bioanal. Chem.* **2016**, *408* (18), 5021−5030.
(19) Jia, L.; Qian, S. B. *Acc. Chem. Res.* **2021**, *54* (23), 4272−4282.
(20) Ramanathan, A.; Robb, G. B.; Chan, S. H. *Nucleic Acids Res.* **2016**, *44* (16), 7511−7526.
(21) Shanmugasundaram, M.; Senthilvelan, A.; Kore, A. R. *Chem. Rec.* **2022**, *22* (8), No. e202200005.
(22) Chan, S. H.; Whipple, J. M.; Dai, N.; Kelley, T. M.; Withers, K.; Tzertzinis, G.; Corrêa, I. R., Jr.; Robb, G. B. *RNA* **2022**, *28* (8), 1144−1155.
(23) Lapham, J.; Crothers, D. M. *RNA* **1996**, *2* (3), 289−296.
(24) Zhang, H.; He, L.; Cai, L. *Methods Mol. Biol.* **2018**, *1754*, 15−27.
(25) Goyon, A.; Scott, B.; Kurita, K.; Maschinot, C.; Meyer, K.; Yehl, P.; Zhang, K. *Anal. Chem.* **2022**, *94* (2), 1169−1177.
(26) Carrilho, E.; Ruiz-Martinez, M. C.; Berka, J.; Smirnov, I.; Goetzinger, W.; Miller, A. W.; Brady, D.; Karger, B. L. *Anal. Chem.* **1996**, *68* (19), 3305−3313.
(27) Kleparnik, K.; Foret, F.; Berka, J.; Goetzinger, W.; Miller, A. W.; Karger, B. L. *Electrophoresis* **1996**, *17* (12), 1860−1866.
(28) Huber, C. G.; Stimpf, E.; Oefner, P. J.; Bonn, G. K. *LC-GC* **1996**, *14* (February), 114−127.
(29) Roussis, S. G.; Pearce, M.; Rentel, C. *J. Chromatogr. A* **2019**, *1594*, 105−111.
(30) Thayer, J. R.; Barreto, V.; Rao, S.; Pohl, C. *Anal. Biochem.* **2005**, *338* (1), 39−47.
(31) Thayer, J. R., High-Resolution Separation of Oligonucleotides on a Pellicular Anion-Exchange Column. *Thermo Scientific Application note 21996*, 2014.
(32) Gilar, M.; Fountain, K. J.; Budman, Y.; Neue, U. D.; Yardley, K. R.; Rainville, P. D.; Russell, R. J., 2nd; Gebler, J. C. *J. Chromatogr. A* **2002**, *958* (1−2), 167−182.
(33) Gilar, M. *Anal. Biochem.* **2001**, *298* (2), 196−206.
(34) Donegan, M.; Nguyen, J. M.; Gilar, M. *J. Chromatogr. A* **2022**, *1666*, No. 462860.
(35) Huber, C. G.; Oefner, P. J.; Bonn, G. K. *Anal. Chem.* **1995**, *67*, 578−585.
(36) Kuwayama, T.; Ozaki, M.; Shimotsuma, M.; Hirose, T. *Anal. Sci.* **2023**, *39* (3), 417−425.
(37) Barth, H. G.; Boyes, B. E.; Jackson, C. *Anal. Chem.* **1994**, *66* (12), 595−620.
(38) Irvine, G. B.; Irvine, G. B., Determination of molecular size by size-exclusion chromatography (gel filtration). In *Current Protocols in Cell Biology*; Wiley, 2001, *Chapter 5*, Unit 5.5.
(39) Munholland, J. M.; Bright, K. A.; Nazar, R. N. *Anal. Biochem.* **1989**, *178* (2), 320−323.
(40) Lukavsky, P. J.; Puglisi, J. D. *RNA* **2004**, *10* (5), 889−893.
(41) Shimoyama, A.; Fujisaka, A.; Obika, S. *J. Pharm. Biomed. Anal.* **2017**, *136*, 55−65.
(42) Kim, I.; McKenna, S. A.; Viani Puglisi, E.; Puglisi, J. D. *RNA* **2007**, *13* (2), 289−894.
(43) Largy, E.; Mergny, J. L. *Nucleic Acids Res.* **2014**, *42* (19), No. e149.
(44) Gilar, M.; Belenky, A.; Budman, Y.; Smisek, D. L.; Cohen, A. S. *J. Chromatogr. B Biomed. Sci. Appl.* **1998**, *714* (1), 13−20.
(45) Gilar, M.; Bouvier, E. S. P. *J. Chromatogr. A* **2000**, *890* (1), 167−177.
(46) Thayer, J. R.; Wu, Y.; Hansen, E.; Angelino, M. D.; Rao, S. *J. Chromatogr. A* **2011**, *1218* (6), 802−808.
(47) Liu, R.; Ruan, Y.; Liu, Z.; Gong, L. *Rapid Commun. Mass Spectrom.* **2019**, *33* (7), 697−709.
(48) Li, N.; El Zahar, N. M.; Saad, J. G.; van der Hage, E. R. E.; Bartlett, M. G. *J. Chromatogr. A* **2018**, *1580*, 110−119.
(49) Neue, U. D. *HPLC columns: theory, technology, and practice*. Wiley-VCH: New York, 1997.
(50) Gilar, M.; DeLano, M.; Gritti, F. *J. Chromatogr. A* **2021**, *1650*, No. 462247.
(51) Guimaraes, G. J.; Sutton, J. M.; Gilar, M.; Donegan, M.; Bartlett, M. G. *J. Pharm. Biomed. Anal.* **2022**, *208*, No. 114439.
(52) Tuytten, R.; Lemière, F.; Witters, E.; Van Dongen, W.; Slegers, H.; Newton, R. P.; Van Onckelen, H.; Esmans, E. L. *J. Chromatogr. A* **2006**, *1104* (1−2), 209−221.
(53) Gilar, M.; Neue, U. D. *J. Chromatogr. A* **2007**, *1169* (1−2), 139−150.
(54) Fountain, K. J.; Gilar, M.; Gebler, J. C. *Rapid Commun. Mass Spectrom.* **2003**, *17* (7), 646−653.

(55) Koshel, B.; Birdsall, R.; Chen, W. *J. Chromatogr. B Analyt. Technol. Biomed. Life Sci.* **2020**, *1137*, No. 121906.
(56) Goyon, A.; Zhang, K. *Anal. Chem.* **2020**, *92* (8), 5944−5951.
(57) Apffel, A.; Chakel, J. A.; Fischer, S.; Lichtenwalter, K.; Hancock, W. S. *Anal. Chem.* **1997**, *69*, 1320−1325.
(58) DeLano, M.; Walter, T. H.; Lauber, M. A.; Gilar, M.; Jung, M. C.; Nguyen, J. M.; Boissel, C.; Patel, A. V.; Bates-Harrison, A.; Wyndham, K. D. *Anal. Chem.* **2021**, *93* (14), 5773−5781.
(59) Nguyen, J. M.; Gilar, M.; Koshel, B.; Donegan, M.; MacLean, J.; Li, Z.; Lauber, M. A. *Bioanalysis* **2021**, *13*, 1233.
(60) Birdsall, R. E.; Gilar, M.; Shion, H.; Yu, Y. Q.; Chen, W. *Rapid Commun. Mass Spectrom.* **2016**, *30* (14), 1667−1679.
(61) Birdsall, R. E.; Kellett, J.; Yu, Y. Q.; Chen, W. *J. Chromatogr. B Analyt. Technol. Biomed. Life Sci.* **2019**, *1126−1127*, No. 121773.

https://doi.org/10.1021/acs.analchem.3c02552
Anal. Chem. 2023, 95, 14308−14316